Study of vapourised solvent attack on additive manufacturing part surface

[1] [2] [3] **Prof. Marlon Wesley Machado Cunico, Ph.D. ,** marloncunico@yahoo.com.br
[2]**Prof. Miriam Machado Cunico,Ph.D.**
[1]**Prof. Jonas de Carvalho, Ph.D.**
[1]Universidade de São Paulo campus São Carlos
[2]Concep3d Pesquisas Científicas
[3]Pontificia Universidade Católica do Paraná

Abstract:
The additive manufacturing technologies has been facing an extraordinary growth during that last years, mainly as consequence of the increase of low cost FDM technologies into the marketing. In contrast with that, one of the main disadvantages of this sort of equipment is the final object finishing. For that reason, the main goal of this work is to present and characterise the post-processing which was introduced in the marketing as smoothing. In addition, a concise overview about the theory beneath this process is presented besides an experimental study that evaluates the impact of this process for the main mechanical properties of object.

Key words: *Additive manufacturing, Smoothing process, dimensional evaluation*

1. INTRODUCTION

It is know that the additive manufacturing technologies imply on several benefits for product development, shorting the time for product launch and creating product differentiation. Along the last years, the introduction of low cost equipment into the marketing can be highlighted to result in a significant business growth and popularisation of process.

On the other hand, the main technology applied in low cost equipment is marked to produce poor surface finishing, restricting its application for hobby and prototypes issues. In addition, it is also possible to identify that those low cost products commonly result in low mechanical strength in building direction, creating another barrier for application of this equipment.

For that reason, the main goal of this work is to present and characterise the surface post-process that was introduced by Stratasys in 2003 (Patent) and is known as smoothing process (PRIEDEMAN e SMITH, 2003). A schematic of this process can be seen in Figure 1, where the finishing of the object is provided by a vaporised solvent treatment.

In this proposal, the object is placed in chamber where a vaporised solvent attacks the surface of object. As consequence of the solvent attack the solubilisation of the superficial material occurs in addition to the change of superficial material from solid to liquid phase.

In general way, the main steps of this process are: object exposure, object drying and repeating process. In the object exposure step, the object is inserted in a chamber fulfil of vaporised solvent in a predetermined temperature and pressure. After an exposure time, the object is removed from the vapour chamber to a dry chamber in order to dry the solvent which is impregnated in the object surface and to cure the material which was solubilised by the solvent. By the end, the object is finished and prepared to receive a final surface treatment, when necessary (PRIEDEMAN e SMITH, 2003).

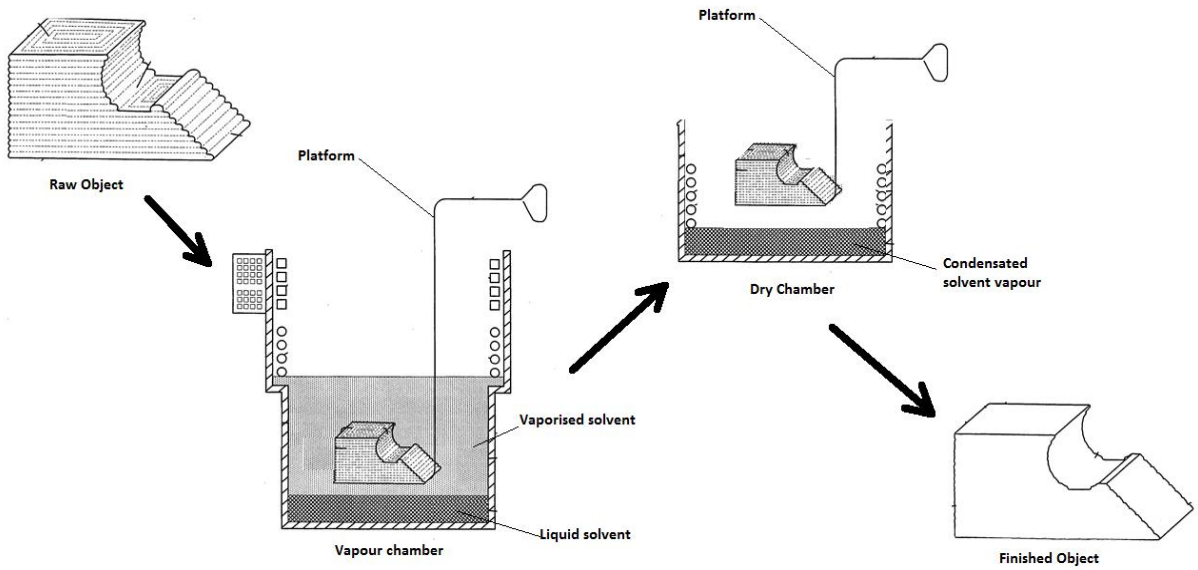

Figure 1 –Schematic of smoothing process based on(PRIEDEMAN e SMITH, 2003)

One example of the result of this process can be seen in Figure 2, where an object which was built in a poor layer resolution (0.35mm) implied on a polished finishing after smoothing process. It is also important to highlight that this situation might be a game changer in the specialised and small scale business segment, whereas the poor quality objects from low cost 3D printers might result in finals part or products.

Figure 2 –Example of object before(a) and after(b) smoothing process

In this process, it is important to highlight that the solvent must be compatible with the object polymeric material which is expected to receive the treatment. For that reason, this work intends to identify the main parameters that are needed to select the suitable solvent for each plastic.

To determine the polymer solubility, the similarity between polymer and solvent chemical structure might be one of the criterion. Nevertheless, the polymer solubility might be also affected by the temperature and reduction of molecular mass of polymeric chain (HANSEN, 1967; BRANDRUP *et al.*, 1999; ODIAN, 2004; CANEVAROLO, 2006).

One of the main approaches to identify the similarity between solvent and polymer is the analysis of the cohesive energy, which indicates the energy that is necessary to segregate one molecule from its environment. In general way, this energy is related to the phase changing so that for liquids, this energy value is associated to the evaporation (Eq. (1)) (HANSEN, 1967; BRANDRUP *et al.*, 1999; ODIAN, 2004; CANEVAROLO, 2006).

$$DEC = \frac{\Delta Hv}{V}\left[cal/cm^3\right] \quad \textbf{(1)}$$

In this way, the solubility between a solute into a liquid might be described by the free energy of mixing (ΔG) which results in a negative variation between the enthalpy (ΔH) and the Entropy (ΔS) in a specific Temperature (T), as presented in Eq. (2) (HANSEN, 1967; BRANDRUP *et al.*, 1999; ODIAN, 2004; CANEVAROLO, 2006)

$$\Delta G = \Delta H - T \cdot \Delta S \quad \textbf{(2)}$$

Therefore, one simplified approach to identify the solubility between polymer and solvent considers the Hildebrand proposal of Enthalpy (Eq. (3)), where: $\delta_1 = \sqrt{DEC_{solvent}}$, $\delta_2 = \sqrt{DEC_{polymer}}$ and the volumetric fraction of solvent and polymers are φ_1 and φ_2 (HANSEN, 1967; BRANDRUP *et al.*, 1999; ODIAN, 2004; CANEVAROLO, 2006).

$$\Delta H = \varphi_1 \cdot \varphi_2 \cdot (\delta_1 - \delta_2)^2 \, | \quad \textbf{(3)}$$

In this case, we can consider that, for amorphous thermoplastics, the solubility occurs when:

$$|\delta_1 - \delta_2| \leq 3.47\left[cal/cm^3\right]^{\frac{1}{2}} \quad \textbf{(4)}$$

In order to evaluate the potential and implications of this process, we selected acetone as solvent and we investigated the main effects of this solvent vapour on low cost FDM object. As result, we could measure the surface roughness decrease as a function of number of exposure passes.

2. MATERIAL AND METHODS

For the experimental analysis of smoothing process, we applied an univariable method where the temperature, object orientation, object material and solvent were the constants. On the other hand, we considered the number of exposure passes and the exposure time as the main variables, while the absorbed solvent, drying ratio, surface roughness and dimensional distortion were the study responses. In addition, we have also performed the microscopically analysis of transversal section before and after solvent exposure.

In order to do this study, it was selected a specimen geometry that allows us investigating the geometrical distortion in large and small features and performing a tensile test. In addition, the object geometry was also selected to represent a real common application, where occurs the different surface orientations. The schematic of this specimen is presented in Figure 3a, where it is presented the main dimensions that we analysed in this work. In this figure, it is also presented the direction of tensile test and the building orientation.

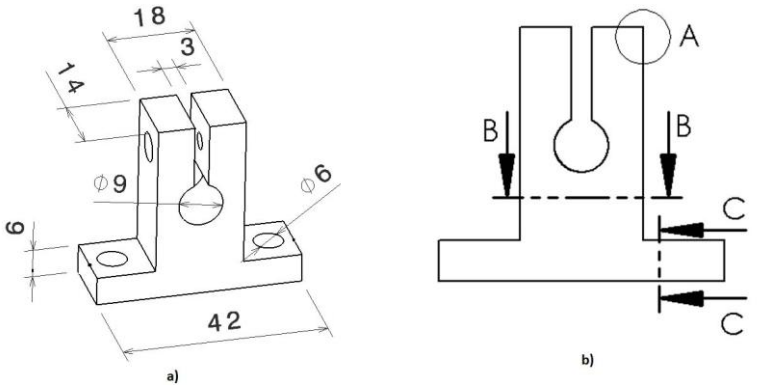

Figure 3 – Scheme of specimen main dimensions and load direction (a) and microscopy analysis areas (b)

For the analysis of the dimensional distortion, we used a 0.01mm error calliper and 6 measurement points for each dimension. Therefore, the geometrical distortion along the surfaces might be identified. At this way, we have also selected one region to analyse the surface finishing of each specimen long the exposure passes (A), as presented in Figure 3b. The section for the microscopic analysis were also presented in order to be evidenced the behaviour of vapour attack on longitudinal (Cut B-B) and transversal (Cut C-C) filaments orientation.

For specimen fabrication, we used a FDM process and natural ABS GP35 with black colour master as material. The main process parameters were remained constants, where layer thickness was 0.4mm; distance between filaments was 0.6 mm; and nozzle diameter was 0.5mm.

For the variation of solubility parameter, we used acetone as solvent, while temperature which were used was 70°C. This case, as the boiling temperature of acetone is 56°C, we ensure that the vapour generation is kept constant along the exposure time.

It is also important to highlight that before each exposure pass, the chamber temperature and solvent volume inside the boiling reservoir were put to the initial condition, where the temperature was 25º and the solvent volume was 10ml. in addition, the temperature ramp rate was defined according to Figure 4. In this figure, it is possible to see that the exposure time after boiling temperature was found to be 4 minutes.

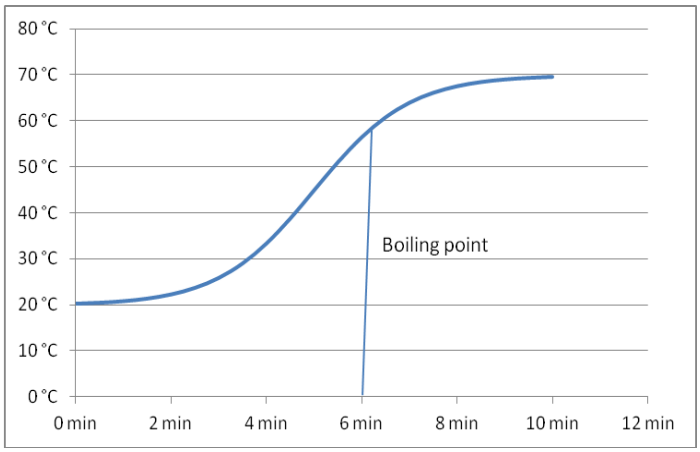

Figure 4 – Increasing temperature ramp curve

Another point that is also important to be highlighted is the drying time. In order the investigate the interferences related to residual solvent into the object. We established drying time equal to 15 minutes into a controlled environment in 25°C and monitored the objet mass along this period. As consequence the amount of solvent that was absorbed by the object could be identified besides the cumulative effect along exposure passes.

In Table 1 is presented the design of experiment which was used , it is also presented the schematic of object orientation with respect to the platform and the solvent reservoir. It is important to note that the exposure passes was defined to have 18 analysis levels, were the behaviour of the same specimen was monitored in all passes. In order to ensure the statistical confidence of this study, we submitted 3 samples to the same procedure.

Table 1 – Design of experiment

	Description
Number of passes	1-18
Exposure time (min)	10 / 15
Temperature (°C)	70
Object Orientation (degree)	 0
Solubility parameter $\lvert\delta_1 - \delta_2\rvert\cdot[MPa\ ]^{\frac{1}{2}}$	1,87
Solvent	Acetone

In the surface finishing analysis, we used an optical microscope and image processing in order to obtain the roughness of surface. For the image processing, we used the software MATLAB, while the image acquisition, we used the optic microscope Digital Avangard Optics AN-E500 (AVANGARD, 2011), which provides until 500x of amplification magnitude. For the gravimetric analysis (drying monitoring), we used an 0.005g error scale.

In Figure 5, it is presented a schematic of the apparatus which we used in this study, where is indicated the position of thermocouples object platform and solvent reservoir. It can also be noted that the chamber is closed in order to force the solvent vapour to attack homogeneously all the object surfaces.

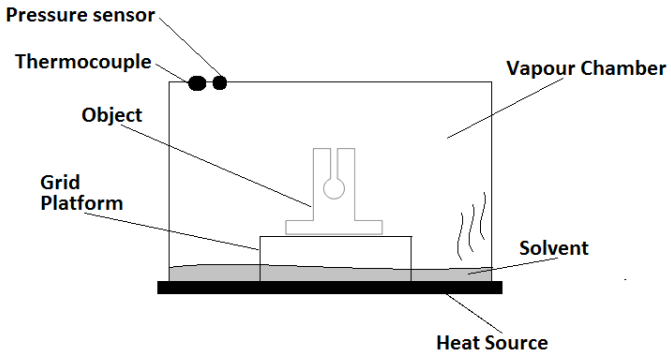

Figure 5 – Scheme of smoothing process experimental study apparatus

In order to ensure the experiment repeatability we established a procedure that consists in 5 steps, exposure, drying, dimensional analysis, surface roughness analysis and microscopy, as it is possible to see in Figure 6.

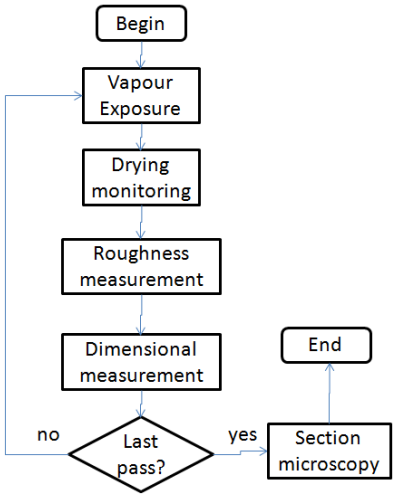

Figure 6 – Experiment flow chart

In this procedure, we included a stabilisation step before performing the tests after smoothing. This step was included to dry the solvent which impregnated the part surface. Otherwise, the properties of specimens would be jeopardised.

It is also important to note that all the specimens that suffered vapour treatment were submitted to microscopic analysis in addition to one specimens which were not exposed to vapour. In this case, these specimens were used as reference to analyze the effects of vapour treatment on the object.

3. RESULTS AND DISCUSSIONS

With respect to the results of experiments, the accumulation of solvent inside the object was evidenced, in addition to the decrease of surface roughness as a function of exposure passes. the dimensional distortion was not possible to be seen for exposure time of 10 min per pass even though the impregnation of solvent inside the objet resulted layers fusion.

On the other hand, severe geometrical distortions and surface disruptures were evidenced for 5 passes with 15 min of exposure per pass, as it is possible to be seen in Figure 7. It is also noted that the specimen become extremely rubbery and the specimen stiffness were jeopardized when absorbed solvent mass were higher than 8%. It might be one cause of distortion.

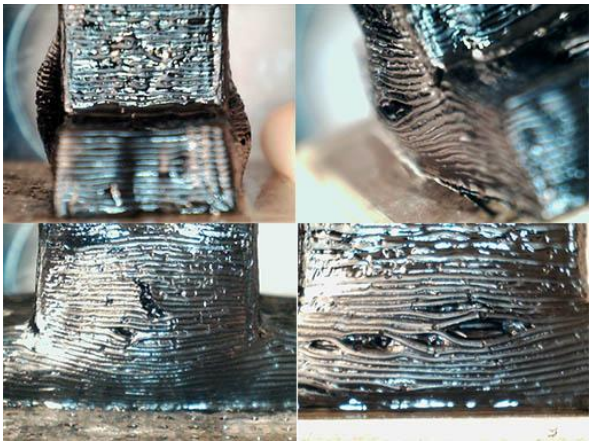

Figure 7 – Distortion resulted from smoothing process with 15 min of exposure per pass

In the gravimetric analysis during exposure and drying stages, the accumulation of solvent inside the specimen was evidenced as it is possible to see in Figure 8.

In this figure, we have also analysed the behaviour of solvent absorption as a function of number of passes and exposure time per pass. As result, we found that the absorption tends to increase according Eq. (5) and 84% of confidence.

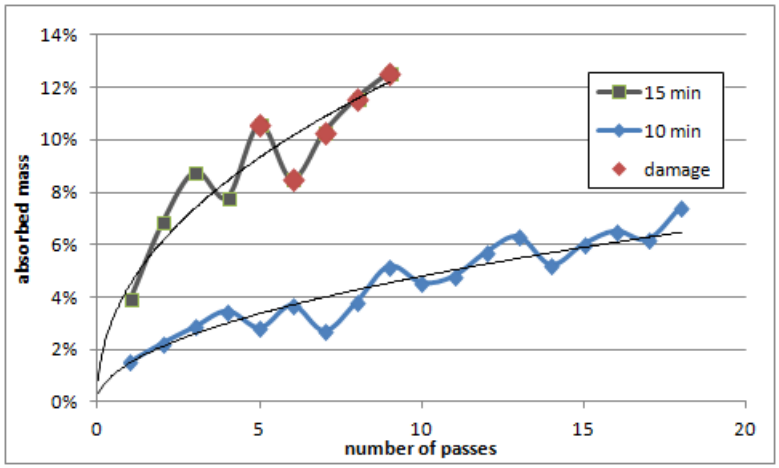

Figure 8 – Gravimetric analysis

$$A = t \cdot 7.5 \cdot 10^{-4} \cdot n^{t \cdot 8.61 \cdot 10^{-2}} \quad \textbf{(5)}$$

Where:

A is the proportional absorbed mass (%)
n is the number of exposure passes
t is the exposure time per pass (min)

Additionally, this figure also shows the moment when the specimen damages started, evidencing that the distortion might occur as result of high levels of absorbed solvents. In this case, it is possible to correlate such distortions with the absorbed mass higher than 8 %. However, further studies are still needed to better understand this behaviour.

On the other hand, it was also possible to see that the drying stage tends to stagnate and has a Logarithmic decay, as it is possible to see in Figure 9.

In spite of this indication, this study only considered a single specimen geometry and the absorption ratio is probably co-dependent to exposure surface area. Additionally, the vapour attack is also dependent to vapour generation rate and exposure temperature, as the solubility depends on system entropy. Therefore, further studies are still needed in order to identify a generalised absorption rate equation.

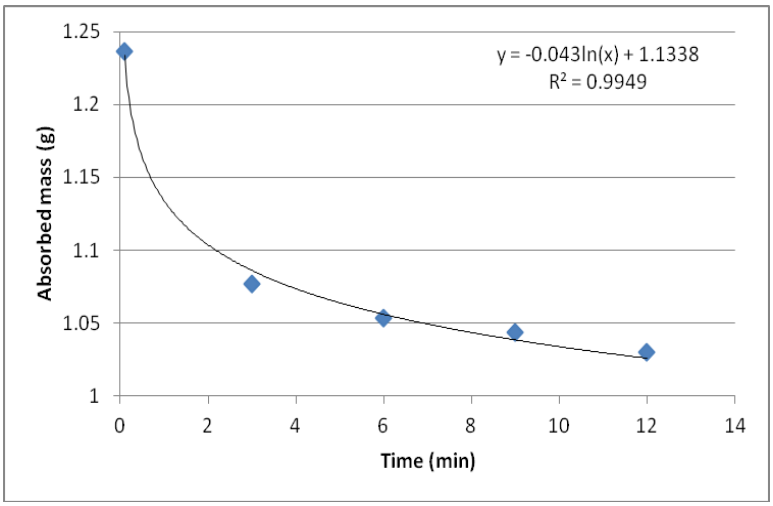

Figure 9 – Drying Gravimetric analysis of 13rd pass with 10 min of exposure time

With respect to surface roughness, it was possible to identify the decrease of surface roughness as a function of the number of passes, as presented in Figure 10. In this case, the total roughness decrease was up to 71%, evidencing the benefit of use of such method for surface smoothing.

In spite the roughness decrease fast with longer exposure time, the stagnation occurs in few steps, even though the occurrence of specimen damage.

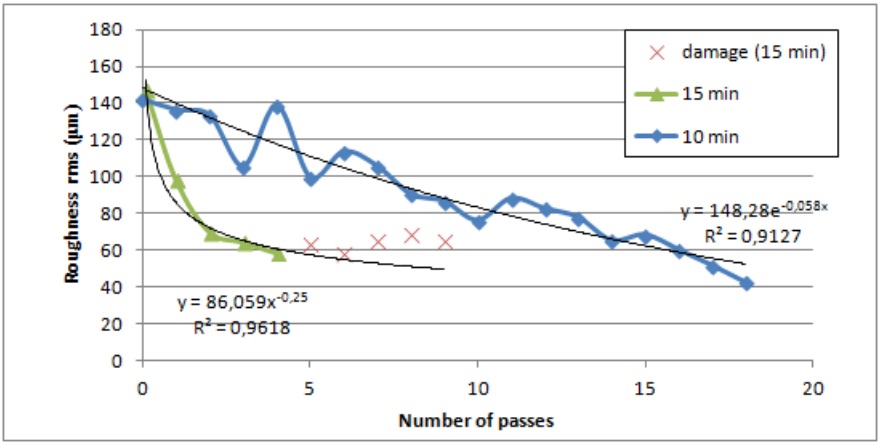

Figure 10 – Surface Roughness as a function of number of passes

Additionally, Figure 11 indicates that the layer separation become less evident, and the flexibility on surface tends to indicate better homogeneity. It might indicate that the strength between layers increased, however, further studies still needed to be performed in order to evidence such hypothesis.

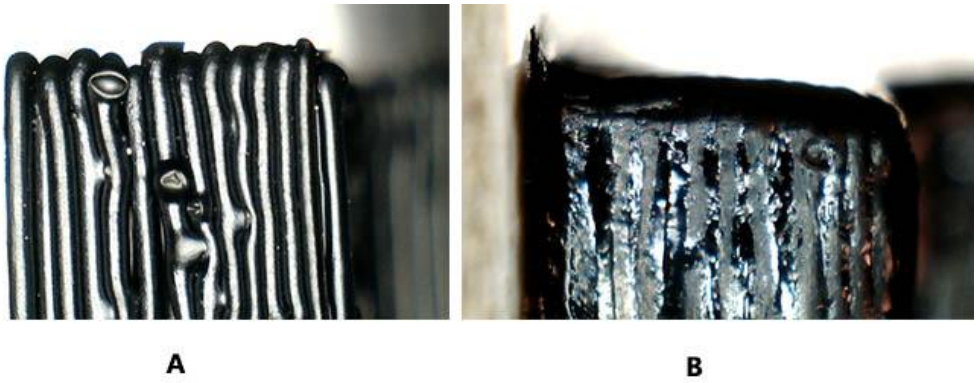

Figure 11 – Comparison between object surface at before smoothing process (A) and after 16th pass (B) with 10 min of exposure

Another event that was also possible to be seen is relative to the method and apparatus that was used. Using the current apparatus layout, the surface smooth started from the bottom of the object, as presented in Figure 12. Therefore, there are indications that the object orientation imply on strong effects on final object results. In this way, there are still several aspects of this finishing process to be investigated in future studies.

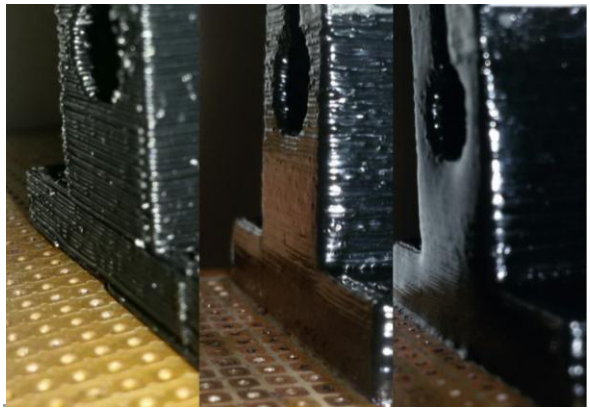

Figure 12 – Progress of smoothing along the object

With reference to the dimensional distortion of object as a function of vapour attack, no relevant dimensional distortion was possible to be correlated with such process through the used measurement method. Nonetheless, the straightness was found to be reduced in small size geometries, as presented in Figure 13. It indicates that geometrical distortions might be caused by vapour attack process.

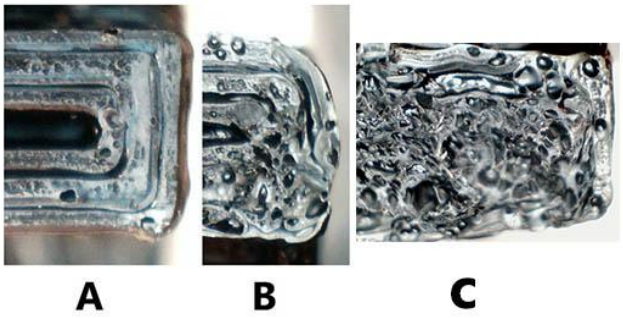

Figure 13 – Comparison between straight surface before vapour exposure(A) and after vapour attack with 10 min of exposure (B) and after 15 min of exposure (C)

In addition, this figure also indicates the how deep the vapour attack penetrated inside the specimen when exposure to vapour during 15 min per pass. It is possible to see that the internal structure of object was affected and the voids created by airgap strategy cause bubbles.

Through the microscopic analysis of specimen sections, we can identify that the solvent welded filaments and layer along the depth of around 1mm. This situation might be evidenced in Figure 14. As result, it indicates that the increase

of mechanical strength might be a secondary result of vapour attack. And if this hypothesis would be true, the anisotropic behaviour of additive manufacturing objects might be reduced by vapour attack process.

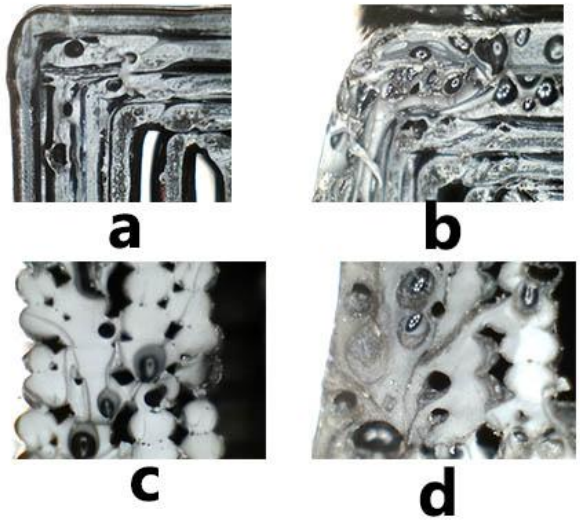

Figure 14 – Analysis of solvent attack depth in longitudinal and transversal specimen sections, where a) longitudinal section before attack; b) longitudinal section after attack (18 passes with 10 min of exposure); c) transversal section before attack; d)transversal section after attack (18 passes with 10 min of exposure)

On the other hand, the analysis of the section of specimen which were exposed to solvent vapour during 15 min per pass indicated internal disruptures. This might be a consequence of gas expansion inside specimen besides low stiffness resulted from solvent attack.

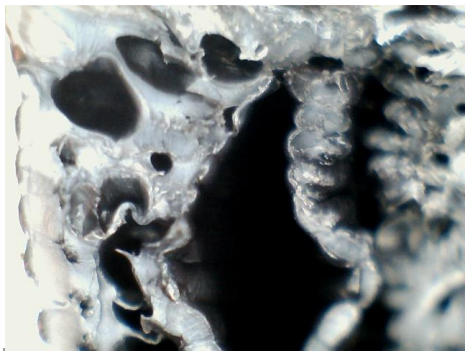

Figure 15 – Analysis of solvent attack depth in longitudinal specimen sections after 9 passes with duration of 15 min

Moreover, this work highlighted the benefits of solvent vapour attack in FDM objects in addition to the disadvantages an issues inherent to this process. This process was shown to be remarkable to improve object aesthetic and potential increase mechanical strength of FDM object. Nevertheless, there are still several challenges to be overcome in this process in order to optimize its potential application.

4. CONCLUSIONS

As conclusion of this work, we evidenced that solvent vapour attack or smoothing process might reduce the overall roughness in 70% . In addition, it was also observed the absorption of solvent inside the specimen and the accumulation of this solvent has grown in each time that the object was exposed to vapour attack.

It was also seen that even though part of absorbed solvent vaporised during a drying phase, the mass decay tend to be logarithm and leads to an stagnation point.

Along this work, it was also found that the dimensional distortion has no relevant variation even though the straightness of small geometries might be jeopardized. In addition, long exposure time were evidenced to result in severe distortion of objects, stiffness and hardness decrease.

By the end, it was also evidenced that the vapour attack with 10 min of exposure per pass penetrated around 1 mm inside the object and fused either layers and filaments in a surface shell. It might indicated an improvement of mechanical strength and reduction of anisotropic behaviour of components.

In spite of this results, this work is found in a preliminary stage and further studies must be done in the future in order to better understand the benefits and disadvantages of such process.

5. ACKNOWLEDGMENTS

The authors would like to thank the CNPQ for financial support, as well as the Department of Mechanical Engineering of the University of São Paulo,(campus São Carlos) and the Research department of Concep3D, for providing access to infrastructure and Laboratories.

6. REFERENCES

AVANGARD. Avangard Optics AN-E500 eScope 500x USB 2.0 Mega Pixel Digital Microscope. Avangard Optics. 2011. Disponível em: <www.bhphotovideo.com/>. Acesso em: agosto de 2011.

BRANDRUP, J., E. H. IMMERGUT, *et al.*, Eds. **Polymer Handbook**: John Wiley & Sons, Inc., p.2370 ed. 1999.

CANEVAROLO, S. V. **Ciência dos polímeros: um texto básico para tecnólogos e engenheiros**: Artliber. 2006

HANSEN, C. M. The three dimensional solubility parameter. **Danish Technical: Copenhagen**, p.14. 1967.

ODIAN, G. **Principles of Polymerization**: John Wiley & Sons, Inc. 2004. 840 p.

PRIEDEMAN, W. R. e D. T. SMITH. Smoothing method for layered deposition modeling. USA: Stratasys, Inc. 2003.